Cardiovascular Research Advance Access published March 14, 2016

Cardiovascular Research
doi:10.1093/cvr/cvw026

Selective phosphorylation of PKA targets after β-adrenergic receptor stimulation impairs myofilament function in *Mybpc3*-targeted HCM mouse model

Aref Najafi[1,2]*, Vasco Sequeira[1], Michiel Helmes[1], Ilse A.E. Bollen[1], Max Goebel[1], Jessica A. Regan[1], Lucie Carrier[3,4], Diederik W.D. Kuster[1], and Jolanda Van Der Velden[1,2]

[1]Department of Physiology, Institute for Cardiovascular Research (ICaR-VU), VU University Medical Center Amsterdam, Netherlands; [2]ICIN—Netherlands Heart Institute, Utrecht, The Netherlands; [3]Institute of Experimental Pharmacology and Toxicology, Cardiovascular Research Center, University Medical Center Hamburg—Eppendorf, Hamburg, Germany; and [4]DZHK (German Centre for Cardiovascular Research), Partner Site Hamburg/Kiel/Lübeck, Germany

Received 8 July 2015; revised 21 December 2015; accepted 22 January 2016; online publish-ahead-of-print

Time for primary review: 43 days

This manuscript was handled by a Consulting Editor.

Aims Hypertrophic cardiomyopathy (HCM) has been associated with reduced β-adrenergic receptor (β-AR) signalling, leading downstream to a low protein kinase A (PKA)-mediated phosphorylation. It remained undefined whether all PKA targets will be affected similarly by diminished β-AR signalling in HCM. We aimed to investigate the role of β-AR signalling on regulating myofilament and calcium handling in an HCM mouse model harbouring a gene mutation (G > A transition on the last nucleotide of exon 6) in *Mybpc3* encoding cardiac myosin-binding protein C.

Methods and results Cardiomyocyte contractile properties and phosphorylation state were measured in left ventricular permeabilized and intact cardiomyocytes isolated from heterozygous (HET) or homozygous (KI) *Mybpc3*-targeted knock-in mice. Significantly higher myofilament Ca^{2+} sensitivity and passive tension were detected in KI mice, which were normalized after PKA treatment. Loaded intact cardiomyocyte force–sarcomere length relation was impaired in both HET and KI mice, suggesting a reduced length-dependent activation. Unloaded cardiomyocyte function revealed an impaired myofilament contractile response to isoprenaline (ISO) in KI, whereas the calcium-handling response to ISO was maintained. This disparity was explained by an attenuated increase in cardiac troponin I (cTnI) phosphorylation in KI, whereas the increase in phospholamban (PLN) phosphorylation was maintained to wild-type values.

Conclusion These data provide evidence that in the KI HCM mouse model, β-AR stimulation leads to preferential PKA phosphorylation of PLN over cTnI, resulting in an impaired inotropic and lusitropic response.

Keywords Calcium handling • Contractility • Hypertrophic cardiomyopathy • β-adrenergic signalling

1. Introduction

Hypertrophic cardiomyopathy (HCM) is the most frequently occurring inherited cardiac disorder, with a prevalence of 1:200 in the general population.[1] HCM is characterized by (asymmetrical) left ventricular (LV) hypertrophy, diastolic dysfunction, cardiomyocyte disarray, and cardiac fibrosis.[2,3] Mutations in genes encoding sarcomeric proteins cause HCM,[3,4] with mutations in genes *MYH7* and *MYBPC3* encoding myosin heavy chain (MHC) and cardiac myosin-binding protein C (cMyBP-C), respectively, being the most frequent cause of HCM.[5]

A desensitized cardiac β-adrenergic receptor (β-AR) signalling pathway,[6] which is a hallmark of the failing heart, has been identified in patients with HCM.[7] Besides desensitization of the β-AR pathway, a reduced number of β-receptor binding sites have been reported in patients suffering from HCM.[8] As a consequence, diminished downstream β-AR signalling may occur, leading to a lower protein kinase A (PKA)-mediated protein phosphorylation.[9,10] PKA-mediated phosphorylation of myofilament proteins [e.g. cardiac troponin I (cTnI) and cMyBP-C and Ca^{2+}-handling proteins (e.g. phospholamban (PLN)] mediates positive inotropic and lusitropic cardiac effects.[11,12] In addition,

* Corresponding author. Department of Physiology, VU Medical Center, O2 building, 12W-23 De Boelelaan 1118, 1081 HV Amsterdam, The Netherlands. Tel: +31 627339912 a.najafi@vumc.nl

phosphorylation of cTnI reduces myofilament Ca^{2+} sensitivity, and cMyBP-C phosphorylation accelerates cross-bridge cycling, both of which lead to enhancement of the relaxation rate.[12,13] The phosphorylation of PLN increases the activity of SR Ca^{2+} adenosine triphosphate (ATP)ase-2 (SERCA2a) pump and thereby the rate of cardiac relaxation.[11] Due to increased Ca^{2+} uptake upon β-AR stimulation, a higher SR Ca^{2+} content will be reached, which is available for subsequent contraction, leading finally to an enhancement of contractile performance.[11]

The myofilament proteins cMyBP-C and cTnI are relatively highly phosphorylated in snap-frozen cardiac tissue from healthy individuals, whereas the phosphorylation level is lower in heart tissue from patients with HCM.[9,10] Similarly, low PLN phosphorylation levels have been reported in transgenic HCM mouse models and in patients with heart failure (HF).[14,15] The functional consequences of disturbed β-AR signalling and reduced PKA-mediated phosphorylation are shown in the blunted increase in contractile response following isoproterenol administration, a β-AR agonist.[16] β-AR-mediated increases in inotropy and lusitropy require the concerted phosphorylation of targets at multiple subcellular localizations. Spatial and temporal intracellular targeting of PKA is regulated through a set of A-kinase anchoring protein complexes (AKAPs).[17]

We hypothesized that this coordinated PKA-mediated phosphorylation is disturbed in HCM disease pathology. Therefore, we investigated the effect of β-AR stimulation on myofilament and Ca^{2+} handling in a HCM-associated mouse model. The experiments were performed in an *Mybpc3*-targeted knock-in mouse model, which carries a heterozygous (HET) or a homozygous (KI) *Mybpc3* point mutation (G > A transition) on the last nucleotide of exon 6.[18] The single mutation resulted in low levels of mRNA and less cMyBP-C protein expressions,[18] similar to earlier findings in human HCM myocardial tissue.[10] This mutation is associated with a severe HCM phenotype and poor prognosis in humans.[5] The HET mice are comparable to pre-hypertrophic mutation carriers, with some degree of diastolic impairments,[18] whereas the HCM phenotype (e.g. hypertrophy) is most evident in KI mice.

2. Methods

2.1 Animal model

An expanded version of the methods section can be found in the online supplemental information. Experiments were performed in accordance with the Guide for the Animal Care and Use Committee of the VU University Medical Center (VUmc) and with approval of the Animal Care Committee of the VUmc (DEC-number FYS 11-02 and FYS 12-03) and conform the guidelines from Directive 2010/63/EU of the European Parliament on the protection of animals used for scientific purposes. In total, 58 mice (age 13 weeks at the time of experiment) of both sexes were included in the study: wild-type (WT, $n = 21$), HET ($n = 19$), and KI ($n = 18$) *Mybpc3*-targeted knock-in mice on a Black Swiss genetic background.[18]

2.2 Force measurements on single membrane-permeabilized myocytes

Cardiomyocytes were chemically permeabilized by incubation for 5 min in relaxing solution containing 0.5% (v/v) Triton X-100 and glued between a force transducer and a piezoelectric motor, as described previously.[9]

2.3 Titin isoform composition and phosphorylation

Titin isoform composition was analysed in mice LV homogenates, using a vertical Hoefer SE600 gel system (Hoefer Inc., USA) with a 1% agarose gel, as described previously.[19] Changes in isoform composition were calculated as a ratio of N2BA:N2B. Human soleus (containing ~3.7 MDa N2A isoform) was used as a standard. To determine the phosphorylation of titin, the gel was stained with ProQ Diamond phosphostain (Molecular Probes) for 60 min, washed, and subsequently stained with SYPRO Ruby (Molecular Probes). Titin phosphorylation is expressed as phosphorylated titin (i.e. summed N2B and N2BA values) over total titin protein level.

2.4 MHC isoform composition

Relative MHC content was determined in LV tissue from WT, HET, and KI mice, as described previously.[20] Briefly, MHC isoforms were separated on a 6% acrylamide resolving gel and a 3% stacking gel using an SE600 Hoefer gel system at 32 mA constant current. Human atrial homogenates, containing both α- and β-MHC, were used as a standard. Subsequently, the gels were stained using SYPRO® Ruby, and MHC isoforms were determined.

2.5 Intact cardiomyocyte isolation

Intact cardiomyocytes were isolated, as described previously.[21]

2.6 Force–sarcomere length (FSL) relation

Intact cardiomyocytes were glued on an approximately 60° short glass fibre, which was placed on a force transducer and a piezo motor (long fibre). Once the cell was attached to the glass fibres, the cardiomyocyte was lifted up. Pre-load was applied by stretching the cardiomyocyte using the piezo motor, resulting in diastolic as well as in systolic FSL relation. Finally, to normalize the slope of FSL, we calculated the ratio of the systolic and diastolic FSL relation, which is the amount of force produced per unit increase in SL.

2.7 Cardiomyocyte shortening and Ca^{2+} handling

Unloaded cardiomyocyte measurements were performed as described previously.[22] To investigate the β-AR-stimulated signalling response of the cardiomyocyte, we stopped the continuous perfusion with HEPES buffer (HB) and immediately started perfusion with isoprenaline (ISO; 100 nmol/L in HB, Sigma-Aldrich; Supplementary material online, *Table S1*).

2.8 Protein phosphorylation analysis

Cardiac TnI phosphorylation status of frozen heart tissue samples as well as that of the isolated cardiomyocytes from baseline (BL) and ISO conditions was analysed using one-dimensional sodium dodecyl sulphate polyacrylamide-bound Mn^{2+}-phos-tag gel electrophoresis and western blotting, as described previously.[23] It is important to note that LV frozen protein homogenates are from tissue which was immediately collected upon excision, whereas intact cardiomyocytes were enzymatically isolated and subsequently a part was stored for protein homogenization and phos-tag analysis. Different patterns in cTnI phos-tag analysis between frozen LV and isolated cardiomyocytes might be caused by loss of phosphorylation during the enzymatic isolation procedure.

Western blotting analysis of site-specific phosphorylation of PLN at the serine (Ser)-16 site, PKA regulatory subunit II (PKA-RII) as well as catalytic (PKAcat) subunit expression and cMyBP-C Ser-302 phosphorylation levels were performed using antibody against PLN phospho Ser-16 (Badrilla, A010-12), PKA-RII (Abcam, ab38949), PKAcat subunit (Enzo Life Sciences, P22694), and Ser-302 phospho antibody (a gift from Dr Sakthivel Sadayappan, Loyola University Chicago), respectively. The signals were normalized for α-actinin (Sigma-Aldrich, A7811), α-tropomyosin (Sigma Aldrich, T9283), and cMyBP-C (Santa Cruz Biotechnology, 137180 Clone E7). The pentameric as well as monomeric isoforms of PLN were detected using the antibody against phosphorylated Ser-16 site. Both pentameric and monomeric isoforms of PLN signals were separately normalized for total PLN (Abcam, ab86930) as well as α-actinin levels and finally summed as one PLN-phosphorylated Ser-16 value. The phosphorylation of threonine (Thr)-17 of PLN (Badrilla, A010-13AP) was also analysed, which was normalized for total PLN expression. PKA-RII, PKAcat, and cMyBP-C expression signals were normalized to α-actinin levels, whereas the Ser-302 cMyBP-C phosphorylation level was corrected for α-tropomyosin.

2.9 Data analysis

Data analysis and statistics were performed using Prism version 6.0 (GraphPad Software, Inc., La Jolla, CA, USA). Data are presented as mean ± SEM of all single cardiomyocytes per mice group. Data were tested for normality by Kolmogorov–Smirnov normality test. When data were distributed normally and in the case of testing one variable in more than two groups, samples were compared using one-way analysis of variance (ANOVA); in the case of two or more variables, the data were compared using a two-way ANOVA. If a significant value in two-way ANOVA was detected, a Holm–Sidak multiple comparison *post hoc* test was performed to identify significance within multiple groups. Significance was accepted when $P < 0.05$.

3. Results

3.1 Higher myofilament Ca^{2+} sensitivity in KI-permeabilized cardiomyocytes

To assess myofilament Ca^{2+} sensitivity of force, force–Ca^{2+} relations were performed at SL 1.8 μm (*Figure 1A*) for all frozen LV samples. Myofilament Ca^{2+} sensitivity was significantly higher in KI (i.e. lower EC_{50}) than in WT mice (*Figure 1A* and *B* and *Table 1*), whereas EC_{50} value in HET mice failed to reach levels of statistical significance ($P = 0.06$). As PKA-mediated phosphorylation of cTnI exerts a dominant regulatory role in the reduction of myofilament Ca^{2+} sensitivity,[24] phos-tag gel analyses were performed to study the distribution of phosphorylated cTnI forms [un-(0P), mono-(1P), and bis-(2P); *Figure 1C*] in LV frozen samples. As illustrated in *Figure 1D*, a significant reduction in the 2P form of cTnI was detected in both HET and KI samples, as well as a higher 0P band particularly in KI mice. To investigate the underlying mechanism of hypophosphorylated cTnI in HCM mice, western blot analysis was performed to detect PKA-RII and PKAcat subunit expression. Interestingly, we found a significantly higher PKA-RII expression in KI mice (Supplementary material online, *Figure S1A*), whereas PKAcat expression did not differ among groups (Supplementary material online, *Figure S1B*). Consequently, PKA-RII/PKAcat ratio was significantly higher in KI when compared with WT and HET counterparts (*Figure 1E* and *F*).

In order to confirm that the lower EC_{50} in KI cardiomyocytes is due to cTnI hypophosphorylation, permeabilized cardiomyocyte measurements were performed following incubation with exogenous PKA. PKA normalized the force–Ca^{2+} relation in KI to WT levels (*Figure 1G* and *H*). It is noteworthy that cells treated with exogenous PKA showed a higher maximal force (F_{max}) than untreated cells in all groups (*Table 1*). In line with the previous study,[18] we also confirmed a significant reduction of cMyBP-C expression in KI mice when compared with WT and HET mice (*Figure 1I* and *J*).

3.2 Higher passive tension in KI-permeabilized cardiomyocytes

Diastolic dysfunction is an early finding in our HCM-associated mouse model,[22] which recapitulates the situation in both mutation carriers[25] and manifest HCM patients.[26] As passive stiffness of cardiomyocytes may underlie diastolic dysfunction, passive tension (F_{pas}) was assessed in membrane-permeabilized LV tissue at SL ranging from 1.8 to 2.4 μm. F_{pas} over the entire range of SL was significantly higher in KI cardiomyocytes than in WT and HET (*Figure 2A*). To determine whether alterations in titin isoform composition may contribute to the higher F_{pas} in KI, the N2BA/N2B ratio was determined. No significant difference between the groups was found (*Figure 2B*). As phosphorylation of titin by PKA reduces F_{pas},[27] analysis of full titin phosphorylation over total titin expression was performed using ProQ Diamond and SYPRO Ruby staining. No differences in total titin phosphorylation were found between the groups (*Figure 2C*). However, exogenous PKA treatment normalized F_{pas} in KI cardiomyocytes to WT and HET levels (*Figure 2D*), indicating that PKA-mediated titin phosphorylation plays an important role in modulating F_{pas} in KI cardiomyocytes.

3.3 Length-dependent activation of myofilaments

Length-dependent activation (LDA) of sarcomeres was determined by measuring Ca^{2+}-dependent myofilament force production at 1.8 and 2.2 μm SL (*Figure 3A* and *B*). An increase in SL resulted in a significantly higher F_{max} and Ca^{2+} sensitivity (*Figure 3C* and *D* and *Table 1*) in all groups. Calculating the difference in EC_{50} between SL 1.8 and 2.2 μm (ΔEC_{50}) showed a lower LDA increase in myofilament Ca^{2+} sensitivity in KI ($\Delta EC_{50} = 0.38 \pm 0.08$ μmol/L) than in WT ($\Delta EC_{50} = 0.56 \pm 0.11$ μmol/L), although the difference was not significant ($P = 0.3$). Myofilament Ca^{2+} sensitivity in KI cardiomyocytes normalized to WT levels at both SLs after treatment with PKA (*Figure 3E* and *F* and *Table 1*). Finally, stretching the cardiomyocyte from SL 1.8 to 2.2 μm revealed (before and after PKA treatment) a decrease in nH coefficient in all groups (*Table 1*). No changes were detected in the maximal rate of tension redevelopment at saturating [Ca^{2+}] (max k_{tr}) within mice groups (1.8 vs. 2.2 μm) and between the groups (*Table 1*).

3.4 Reduced intact cardiomyocyte LDA response in KI mice

In addition to LDA measurements in membrane-permeabilized cardiomyocytes, we examined the LDA response in intact cardiomyocytes from WT, HET, and KI mice. Glass fibres were used to attach an intact cardiomyocyte, stretch the cell, and measure force (*Figure 4A*). In individual cardiomyocytes, the FSL relationship was determined, using the slope of diastolic and systolic force against SL (i.e. force produced per unit increase in SL during rest and peak contraction; *Figure 4B* and *C*). The diastolic slope of FSL relation was comparable between the groups

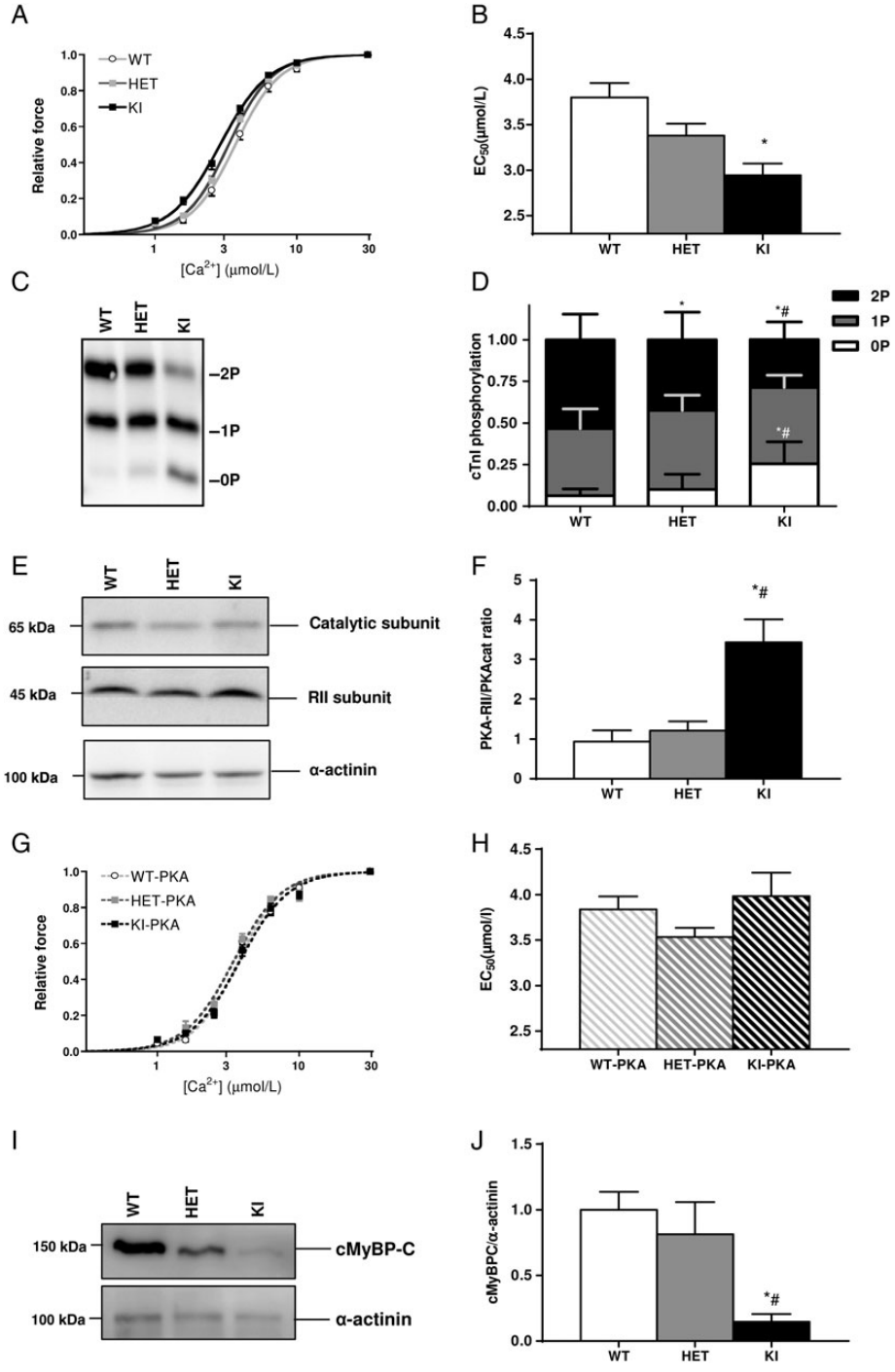

Figure 1 Myofilament Ca^{2+} sensitivity of force. (*A*) The force–Ca^{2+} relation curve of homozygous KI mice [number of mice (N) = 8 and number of cardiomyocytes (n) = 26] was at SL 1.8 μm shifted to the left, indicating a higher sensitivity to [Ca^{2+}]. (*B*) In comparison to WT (n = 9 and n = 28), Ca^{2+} sensitivity (EC_{50}) was significantly higher in KI, indicated as a low EC_{50} value, whereas EC_{50} remained unchanged in heterozygous knock-in mice (HET; N = 9 and n = 26) cells. (*C*) LV samples were separated on a phos-tag acrylamide gel to visualize the distribution of un-(0P), mono-(1P), and bis-(2P) phosphorylation forms of cTnI. (*D*) The relative 1P in KI and 2P phosphorylated forms of cTnI in both HET (N = 10) and KI (N = 9) samples were significantly lower compared with WT (N = 10). (*E*) PKA regulatory subunit II (PKA-RII) and catalytic subunits (PKAcat) expressions were detected and normalized for α-actinin. (*F*) PKA-RII and catalytic subunit ratio was significantly higher in KI (N = 4), compared with WT (N = 3) and HET (N = 4) mice. (*G*) PKA pre-treatment restored the myofilament increase in Ca^{2+} sensitivity in KI (N = 8, n = 24; WT: N = 9, n = 29; HET: N = 9, n = 26) cardiomyocytes, demonstrated as a rightward shift of the force–Ca^{2+} relation. (*H*) PKA treatment resulted in an increase in EC_{50} value in KI (N = 8, n = 24) and HET (N = 9, n = 26) compared to the WT level (N = 9, n = 29). (*I*) Western blot analysis of cMyBP-C expression was corrected for the loading control α-actinin, and subsequently, the values of HET (N = 5) and KI (N = 5) were normalized to WT (N = 4), which was set as 1. (*J*) The relative expression of cMyBP-C was significantly lower than HET and WT mice. *$P < 0.05$ vs. corresponding WT in one-way ANOVA and $^{\#}P < 0.05$ vs. corresponding HET in one-way ANOVA.

Table 1 Effects of exogenous PKA and SL on myofilament function

	No PKA		With PKA		$P_{interaction}$	$P_{treatment}$	P_{LDA}
	SL 1.8 μm	SL 2.2 μm	SL 1.8 μm	SL 2.2 μm			
WT							
F_{max} (kN/m^2)	11.3 ± 0.7	16.9 ± 1.0***	16.0 ± 1.3†	20.5 ± 1.7†***	0.650	<0.001	<0.0001
EC_{50} (μmol/L)	3.8 ± 0.2	3.2 ± 0.1***	3.8 ± 0.1	3.3 ± 0.1***	0.910	0.700	<0.001
nH	3.2 ± 0.2	2.6 ± 0.2***	3.3 ± 0.2	2.7 ± 0.2***	0.880	0.590	0.002
max ktr (s^{-1})	4.1 ± 0.2	4.1 ± 0.2	4.3 ± 0.3	4.6 ± 0.3	0.750	0.160	0.610
HET							
F_{max} (kN/m^2)	10.6 ± 1.0	16.2 ± 1.2***	14.8 ± 1.1†	20.2 ± 1.2†***	0.970	<0.001	<0.0001
EC_{50} (μmol/L)	3.4 ± 0.1*	2.9 ± 0.1***	3.5 ± 0.1	3.0 ± 0.1***	0.840	0.300	<0.0001
nH	3.3 ± 0.2	2.6 ± 0.1***	3.3 ± 0.2	2.4 ± 0.1***	0.460	0.830	<0.0001
max ktr (s^{-1})	4.1 ± 0.3	4.4 ± 0.3	4.1 ± 0.3	4.4 ± 0.4	0.870	0.930	0.350
KI							
F_{max} (kN/m^2)	9.5 ± 1.0	15.3 ± 1.5***	17.7 ± 1.4†	21.9 ± 2.0***†	0.610	<0.0001	0.002
EC_{50} (μmol/L)	2.9 ± 0.1***	2.5 ± 0.1****	3.8 ± 0.1†	3.2 ± 0.1***†	0.630	<0.0001	0.010
nH	2.9 ± 0.1	2.6 ± 0.1	2.9 ± 0.2	2.4 ± 0.1***	0.470	0.690	0.002
max ktr (s^{-1})	3.9 ± 0.4	3.8 ± 0.4	3.6 ± 0.4	3.9 ± 0.3	0.530	0.740	0.800
$P_{genotype}$	F_{max} (kN/m^2)	EC_{50} (μmol/L)	nH	max ktr (s^{-1})			
No PKA	0.313	<0.0001	0.303	0.606			
With PKA	0.313	0.040	0.121	0.081			

WT, wild-type [number of mice $N = 9$ and number of cardiomyocytes (n) = 28]; HET, heterozygous knock-in mice ($N = 9$, $n = 26$); KI, homozygous knock-in mice ($N = 8$, $n = 26$); F_{max}, maximal generated tension; EC_{50}, Ca^{2+} sensitivity [i.e. (Ca^{2+}) at which 50% of F_{max} is reached]; nH, steepness of the force–Ca^{2+} relations; max ktr, maximal rate of tension re-development at saturating [Ca^{2+}].
*$P < 0.05$ vs. corresponding WT.
**$P < 0.05$ vs. corresponding HET.
***$P < 0.05$ vs. corresponding SL 1.8 μm in two-way ANOVA.
$^{\dagger}P < 0.05$ vs. corresponding untreated mice in two-way ANOVA.

(*Figure 4D*), whereas the systolic slope of the FSL response was significantly reduced in both HET and KI mice (*Figure 4E*). Consequently, the systolic/diastolic ratio was significantly lower in both HET and KI groups, indicating a reduced LDA response in intact HET and KI cardiomyocytes.

3.5 Blunted cardiomyocyte response upon ISO treatment in KI mice

Exogenous PKA normalized the deficits in myofilament function in the membrane-permeabilized cardiomyocytes (*Figures 1* and *3*), indicative for disturbed β-AR signalling in our HCM-associated mouse model. To reveal the disturbed β-AR signalling and the contractile response upon β-AR stimulation, isolated intact cardiomyocyte function and phosphorylation were investigated by exposing the cells to the β-AR agonist ISO. Cardiomyocyte contractile function and Ca^{2+} transients were monitored before and after ISO perfusion (*Figure 5A* and *B* and *Table 2*). Diastolic SL was significantly lower in KI compared with WT and HET cardiomyocytes (*Figure 5A* and *Table 2*), as described previously.[22] The maximal re-lengthening velocity, which is the maximum speed reached from peak shortening to baseline SL, was lower in HET mice compared with WT (*Table 2*), whereas other contractile and Ca^{2+}-handling parameters were similar among groups at BL. Similarly, maximal velocity of shortening was slightly reduced only in HET, but not in KI. This reduced shortening velocity (which is the maximal velocity reached at a certain point during relaxation) does not translate into a longer relaxation time (as time to 50% re-lengthening is not changed).

Perfusion with ISO resulted in an increased relative cell shortening in all groups (*Figure 5C* and *Table 2*). Interestingly, cell shortening increased significantly in KI ISO-treated cardiomyocytes when compared with untreated cells; however, the increase after ISO in KI was smaller than that in WT cardiomyocytes, indicating reduced inotropic response in KI upon ISO treatment (*Figure 5C* and *Table 2*). Similarly, an attenuated response to ISO was also seen in other contractile parameters of KI cardiomyocytes, such as cell shortening and maximal re-lengthening velocity (*Figure 5D* and *E* and *Table 2*). To determine whether impaired contractile response to ISO in KI mice might be due to disturbances in Ca^{2+} handling, Ca^{2+} transients were recorded simultaneously. Ca^{2+}-transient amplitude was enhanced upon ISO treatment in all groups (*Figure 5F* and *Table 2*). No changes in Ca^{2+} amplitude and maximal Ca^{2+}-release velocity (*Figure 5G*) were detected among ISO-treated HET, KI, and WT cells. In contrast, maximal Ca^{2+} decay velocity (i.e. the maximal Ca^{2+} re-uptake velocity, which is reached at a certain time during the peak calcium to baseline) was significantly lower in both HET and KI when compared with WT cardiomyocytes after ISO (*Table 2*). Interestingly, despite the blunted response to ISO of maximal re-lengthening velocity and prolonged time to 50% re-lengthening (*Table 2*) in KI mice compared with WT, the time to 50% Ca^{2+} decay and the relaxation index τ were not different between ISO-treated WT, HET, and KI cardiomyocytes (*Figure 5H* and *Table 2*), indicating that Ca^{2+} elimination is preserved in HCM mice. Taking together, the data indicate diminished contractile response of the myofilaments in KI mice upon ISO exposure, whereas the Ca^{2+}-handling function appears to be preserved.

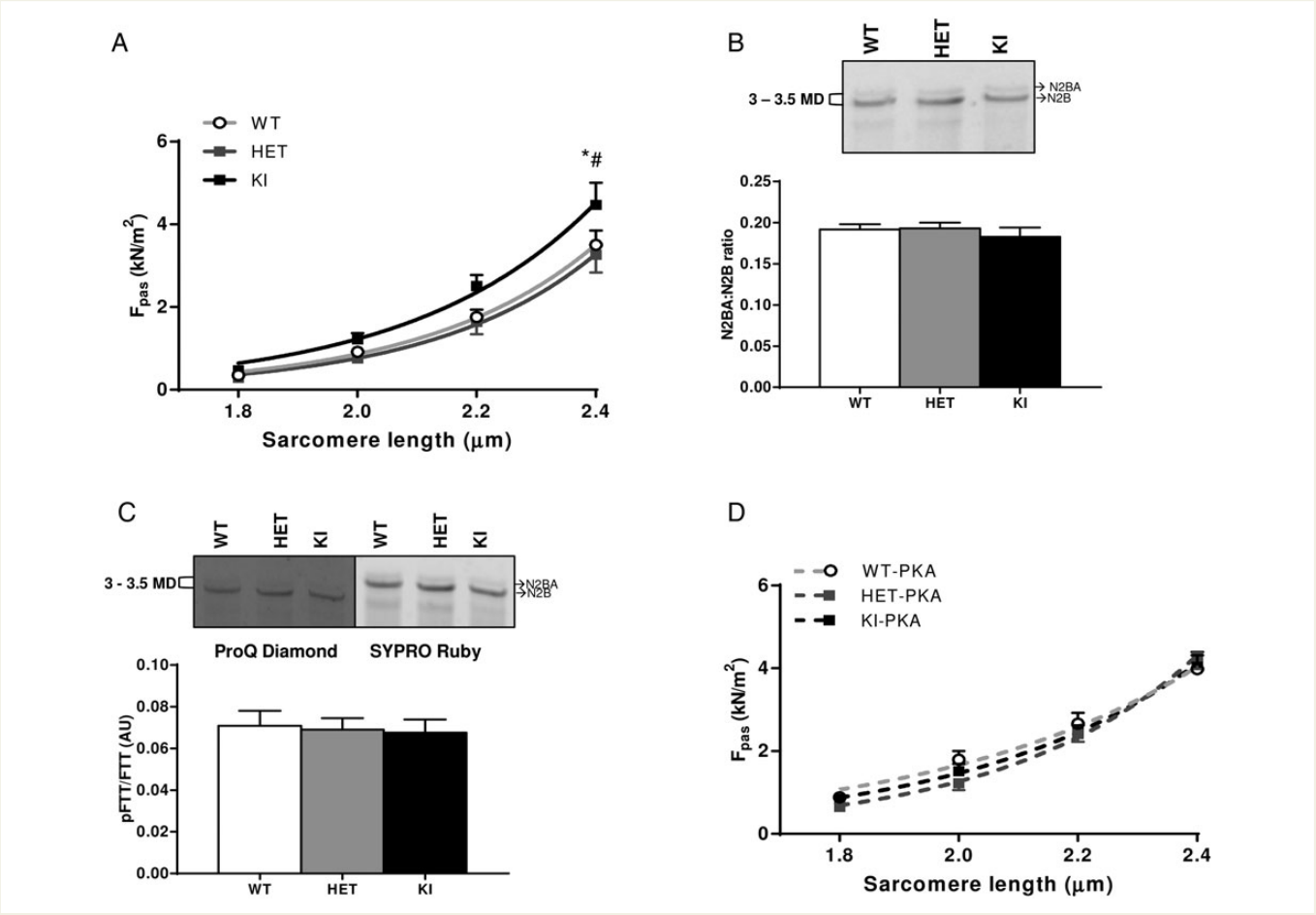

Figure 2 Higher passive tension in homozygous KI mice. (*A*) The mean cardiomyocyte-generated passive force (F_{pas}) over the entire range of SL values was significantly higher in KI [number of mice (N) = 8 and number of cardiomyocytes (n) = 37] mice, compared with WT (N = 10, n = 45) and HET (N = 10, n = 45) mice. (*B*) Separation of N2BA and N2B isoforms of titin on a 1% agarose gel revealed no changes in titin isoform composition between the mice groups (N = 10, 10, and 7 in WT, HET, and KI, respectively). (*C*) The phosphorylated full length titin (N2B + N2BA; N = 4 per group) over total titin analysis revealed no changes between the groups. (*D*) PKA treatment resulted in a reduction of F_{pas} in KI (N = 8, n = 33) cells towards values observed in WT (N = 8, n = 31) and HET (N = 8, n = 35) cells. *$P < 0.05$ vs. corresponding WT in one-way ANOVA and $^{\#}P < 0.05$ vs. corresponding HET in one-way ANOVA.

3.6 Phospholamban, but not cTnI, phosphorylation increased with ISO treatment in KI

As ISO treatment in KI mice led to a similar increase in Ca^{2+} transients as in WT, but had a blunted effect on cardiomyocyte function, we tested whether β-AR stimulation resulted in similar increases in the phosphorylation of cTnI and PLN in the three experimental groups (*Figure 6A–F*). The distribution of phosphorylated cTnI in untreated intact isolated cardiomyocytes did not differ between the groups (Supplementary material online, *Figure S2*). After ISO treatment, the bisphosphorylated forms of cTnI increased significantly in WT and HET cardiomyocytes, whereas in KI mice, the levels were not significantly different from untreated cells (*Figure 6A* and *B*). Similarly, relative cMyBP-C Ser-302 phosphorylation in WT mice increased significantly upon ISO exposure, whereas no alterations were detected in HET and KI cardiomyocytes with ISO treatment (*Figure 6C* and *D*). In contrast, PLN Ser-16 analysis revealed a significant and similar increase in PLN phosphorylation upon ISO in all groups (*Figure 6E* and *F*; $P_{treatment} < 0.05$ in two-way ANOVA). This finding is in line with our observation that Ser-16 phosphorylation of PLN in frozen LV tissue was not different between the groups (Supplementary material online, *Figure S3A* and *B*). Finally, no changes in Thr-17 phosphorylation were observed, which is a Ca2+-calmodulin kinase II (CaMKII) target that was similar between groups before and after ISO treatment (*Figure 6F* and *G*).

4. Discussion

PKA-mediated phosphorylation of several myofilament and Ca^{2+}-handling proteins is an important event upon β-AR stimulation, mediating positive inotropic and lusitropic cardiac effects.[11,12] A reduced phosphorylation of PKA targets has been reported in mouse models and patients with manifest HCM.[10,14,15] Moreover, low cTnI and cMyBP-C phosphorylation has been reported in the myocardium of human HCM patients,[9,10] although recent research has shown that PLN phosphorylation is preserved in patients and a HCM-associated mouse model.[22,28] It is, therefore, not completely known whether a general

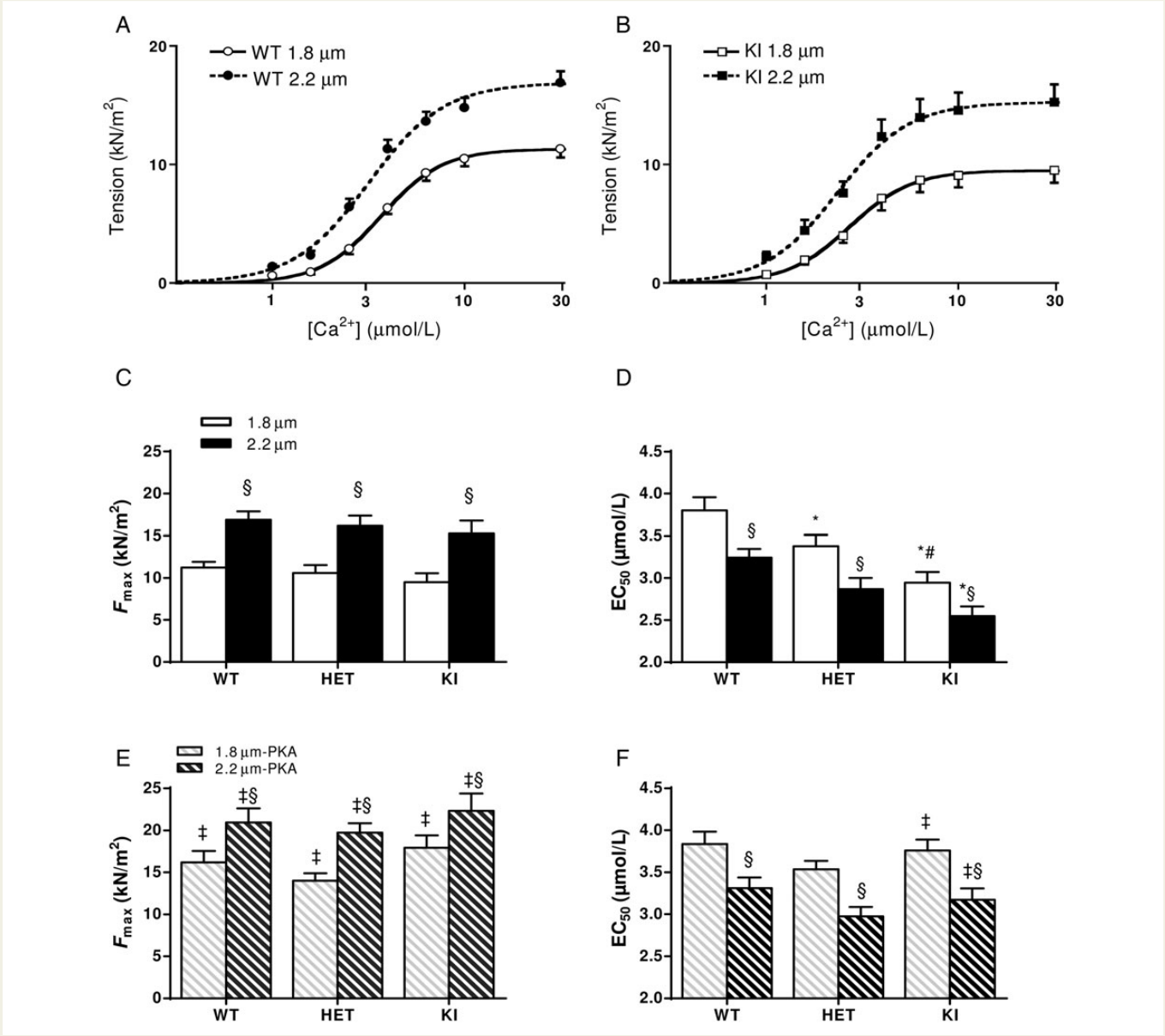

Figure 3 Myofilament length-dependent activation (LDA). (*A* and *B*) Cardiomyocyte force development as a function of $[Ca^{2+}]$ at SL 1.8 and 2.2 μm in WT (number of mice (N) = 9 and number of cardiomyocytes (n) = 28] and homozygous KI ($N = 8$, $n = 26$). (*C*) A similar increase in maximal force (F_{max}) as WT was found after myofilament stretch from 1.8 to 2.2 μm in both HET ($N = 9$, $n = 26$) and KI mice. (*D*) The length-dependent increase in Ca^{2+} sensitivity of force development was slightly lower in KI mice. (*E*) At both SL values, F_{max} was higher in PKA-treated cells compared with untreated cells in all groups (WT: $N = 9$, $n = 29$; HET: $N = 9$, $n = 26$; KI: $N = 8$, $n = 24$). (*F*) No differences in myofilament Ca^{2+} sensitivity were present in PKA-treated cells from the three groups. $^{*}P < 0.05$ vs. corresponding WT in two-way ANOVA; $^{\#}P < 0.05$ vs. corresponding HET in two-way ANOVA; $^{\S}P < 0.05$ vs. corresponding SL 1.8 μm in two-way ANOVA; and $^{\ddagger}P < 0.05$ vs. corresponding untreated SL in two-way ANOVA.

down-regulation of PKA activity or changes in PKA localization occurs in HCM. Our main findings showed: (i) higher myofilament Ca^{2+} sensitivity and passive tension in membrane-permeabilized KI cardiomyocytes which were normalized to WT values after treatment with exogenous PKA; (ii) lower phosphorylated forms of cTnI, but preserved PLN phosphorylation in KI compared with WT hearts; (iii) a blunted increase in cardiomyocyte contractility, but a preserved increase in Ca^{2+} transients in KI compared with WT treated with ISO; and (iv) failure to increase cTnI phosphorylation in KI upon ISO treatment, whereas PLN phosphorylation increased similar to WT. Overall, our study shows that in KI cardiomyocytes, β-AR stimulation preferentially phosphorylates PLN over cTnI, resulting in a blunted myofilament inotropic and lusitropic response.

4.1 Myofilament Ca^{2+} sensitivity and F_{pas} corrected after PKA

Due to improved genetic screening, sarcomere mutations can be detected in the early stage of manifest HCM as well as in family members carrying the mutation. Diastolic dysfunction has been found in mutation carriers even before the onset of hypertrophy in humans.[25] A study in the same HCM mice carrying the same mutation as in the present study

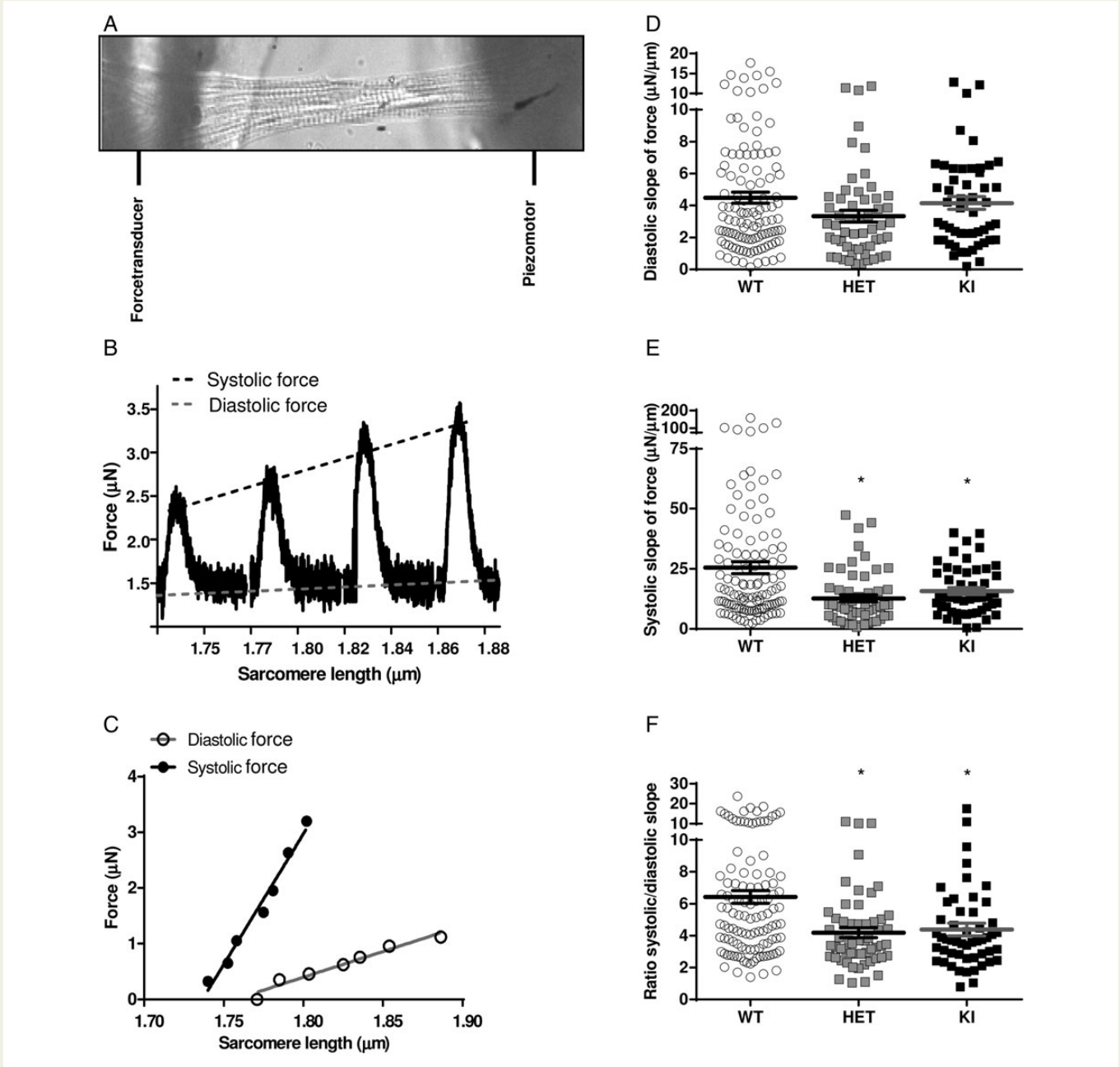

Figure 4 Reduced length-dependent increase in force development per unit increase in SL in both homozygous KI and HET KI, compared with WT mice. (*A*) Intact cardiomyocytes were glued between a force transducer and a piezo motor. (*B*) By stretching a WT cardiomyocyte, we detect a linear FSL relation during diastole as well as systole. (*C*) An increase in both diastolic and systolic FSL was observed upon stretch. (*D*) No differences were found in the diastolic slope of FSL relation among groups. (*E*) In contrast, the systolic slope of FSL was significantly reduced in both HET [number of mice (N) = 9 and number of cardiomyocytes (n) = 55] and KI (N = 10, n = 51), compared with WT (N = 11, n = 113) cells. (*F*) As a consequence, the ratio of systolic over diastolic slope of the FSL relation was significantly lower in both HET and KI than in WT mice. *$P < 0.05$ vs. WT in one-way ANOVA.

reported diastolic dysfunction both in HET and in KI mice.[22] At the myofilament level, diastolic dysfunction can be caused by increased Ca^{2+} sensitivity and/or increased F_{pas}, both of which were observed in KI mice in the present study (*Figures 3D* and *2A*, respectively). In contrast to previous observation in PKA pre-treated trabeculae,[22] the higher myofilament Ca^{2+} sensitivity in KI in the present study was restored to the WT level after PKA treatment (*Figure 1D* and *Table 1*), indicating that the difference in Ca^{2+} sensitivity between KI and WT was mainly due to hypophosphorylation of the sarcomeric proteins rather than the sarcomeric mutation itself. In this study, the distribution of phosphorylated forms of cTnI was significantly lower in both HET and KI mouse hearts (*Figure 1D*). It is well established that phosphorylation of cardiac sarcomeric proteins, particularly cTnI, by PKA reduces myofilament Ca^{2+} sensitivity.[29] PKA pre-treatment corrected the myofilament Ca^{2+} sensitivity, particularly in KI cardiomyocytes, to values observed in WT cells. PKA had no additional effect in WT cells (*Figure 1H*), which can be explained by the relatively high level of bisphosphorylated cTnI (*Figure 1C* and *D*) in WT hearts. Wijnker *et al.*[30,31] revealed that the

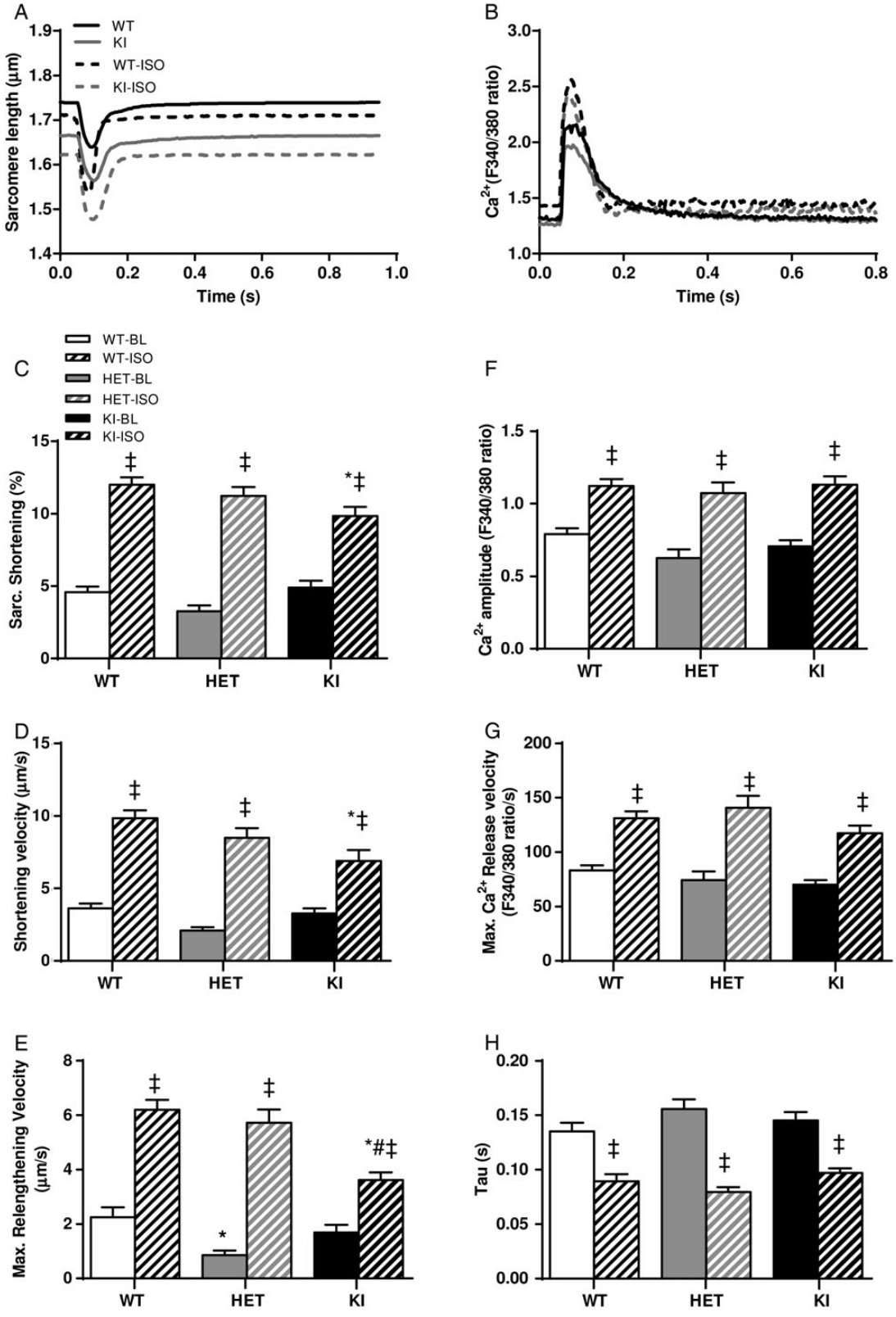

Figure 5 Impaired cardiomyocyte function in homozygous KI upon ISO. (*A* and *B*) Cardiomyocyte shortening and Ca^{2+} transients at baseline (BL) and during ISO treatment are illustrated. (*C*) Less cell shortening was detected in KI [number of mice (N) = 10 and number of cardiomyocytes (n) = 45] compared with WT ($N = 11$, $n = 56$) after ISO perfusion. (*D* and *E*) The cardiomyocyte shortening and maximal (Max.) re-lengthening velocity were significantly lower in KI compared with WT after ISO. (*F* and *G*) The Ca^{2+} amplitude and maximal kinetics of Ca^{2+} release and reuptake were comparable between the groups. (*H*) Similarly, the relaxation index τ, obtained from the Ca^{2+} transient, remained unchanged in both HET KI ($N = 9$, $n = 42$) and KI mice compared with WT. $^{*}P < 0.05$ vs. corresponding WT in two-way ANOVA; $^{\#}P < 0.05$ vs. corresponding HET in two-way ANOVA; and $^{\ddagger}P < 0.05$ vs. corresponding untreated mice in two-way ANOVA.

Table 2 Blunted myofilament response upon β-AR stimulation in KI cardiomyocytes

	BL			ISO				$P_{interaction}$	$P_{genotype}$	$P_{treatment}$
	WT	HET	KI	WT	HET	KI	N/n			
Diastolic SL (μm)	1.73 ± 0.01	1.78 ± 0.01*	1.65 ± 0.01***	1.71 ± 0.01	1.77 ± 0.01*	1.63 ± 0.01***	12/54–10/40–10/45	0.890	<0.0001	0.020
Shortening velocity (μm/s)	−3.6 ± 0.3	−2.1 ± 0.2	−3.3 ± 0.3	−9.9 ± 0.5***	−8.5 ± 0.7***	−6.9 ± 0.8****	12/54–10/40–10/45	0.010	0.001	<0.0001
Amplitude shortening (μm)	0.08 ± 0.01	0.06 ± 0.01	0.08 ± 0.01	0.20 ± 0.01***	0.20 ± 0.01***	0.16 ± 0.01******	12/54–10/40–10/45	0.001	0.053	<0.0001
Sarcomere shortening (%)	4.6 ± 0.4	3.3 ± 0.4	4.9 ± 0.5	12.0 ± 0.5***	11.2 ± 0.6***	9.8 ± 0.6****	12/54–10/40–10/45	0.009	0.070	<0.0001
Time to peak shortening (s)	0.053 ± 0.009	0.056 ± 0.002	0.056 ± 0.006	0.049 ± 0.003	0.054 ± 0.002	0.063 ± 0.003	12/54–10/40–10/45	0.526	0.268	0.779
Time to 50% re-lengthening (s)	0.122 ± 0.018	0.143 ± 0.009	0.117 ± 0.009	0.080 ± 0.003***	0.093 ± 0.004***	0.107 ± 0.004	12/54–10/40–10/45	0.127	0.237	<0.0001
Max. re-lengthening velocity (μm/s)	2.24 ± 0.37	0.86 ± 0.17*	1.70 ± 0.27	6.21 ± 0.35***	5.73 ± 0.49***	3.62 ± 0.28******	12/54–10/40–10/45	0.0001	<0.0001	<0.0001
Diastolic Ca^{2+} (F340/380 ratio)	1.34 ± 0.02	1.34 ± 0.05	1.27 ± 0.04	1.44 ± 0.03	1.46 ± 0.06	1.32 ± 0.04***	12/54–10/40–10/45	0.593	0.016	0.006
Systolic Ca^{2+} (F340/380 ratio)	2.12 ± 0.05	1.96 ± 0.10	1.95 ± 0.06	2.55 ± 0.05***	2.53 ± 0.11***	2.43 ± 0.08***	12/54–10/40–10/45	0.673	0.130	<0.0001
Max. Ca^{2+} release velocity	83.3 ± 4.6	74.3 ± 7.8	69.9 ± 4.3	130.8 ± 6.5***	140.8 ± 11.1***	117.5 ± 6.7***	12/54–10/40–10/45	0.312	0.082	<0.0001
Ca^{2+} amplitude	0.79 ± 0.04	0.63 ± 0.06	0.71 ± 0.04	1.12 ± 0.05***	1.07 ± 0.07***	1.13 ± 0.06***	12/54–10/40–10/45	0.484	0.127	<0.0001
Time to peak Ca^{2+} (s)	0.031 ± 0.008	0.019 ± 0.001	0.045 ± 0.013	0.029 ± 0.004	0.019 ± 0.001	0.033 ± 0.006**	12/54–10/40–10/45	0.674	0.022	0.396
Time to 50% Ca^{2+} decay (s)	0.109 ± 0.007	0.119 ± 0.005	0.130 ± 0.013	0.082 ± 0.004***	0.083 ± 0.003***	0.100 ± 0.006***	12/54–10/40–10/45	0.813	0.017	<0.0001
Max. Ca^{2+} decay velocity	−7.9 ± 0.6	−5.0 ± 0.7	−6.8 ± 0.5	−17.5 ± 1.0***	−14.1 ± 1.1****	−13.0 ± 1.0****	12/54–10/40–10/45	0.101	<0.001	<0.0001
τ (s)	0.135 ± 0.008	0.156 ± 0.009	0.145 ± 0.008	0.089 ± 0.007***	0.079 ± 0.005***	0.097 ± 0.004***	12/54–10/40–10/45	0.065	0.418	<0.0001

WT, wild-type [number of mice (N) = 11 and number of cardiomyocytes (n) = 56]; HET, heterozygous knock-in (N = 9, n = 42)mice; KI, homozygous knock-in mice (N = 10, n = 45); BL, baseline; ISO, isoprenaline-treated cardiomyocytes; SL, sarcomere length; Max., maximal.
*$P < 0.05$ vs. corresponding WT.
**$P < 0.05$ vs. corresponding HET in two-way ANOVA.
***$P < 0.05$ vs. corresponding untreated mice in two-way ANOVA.

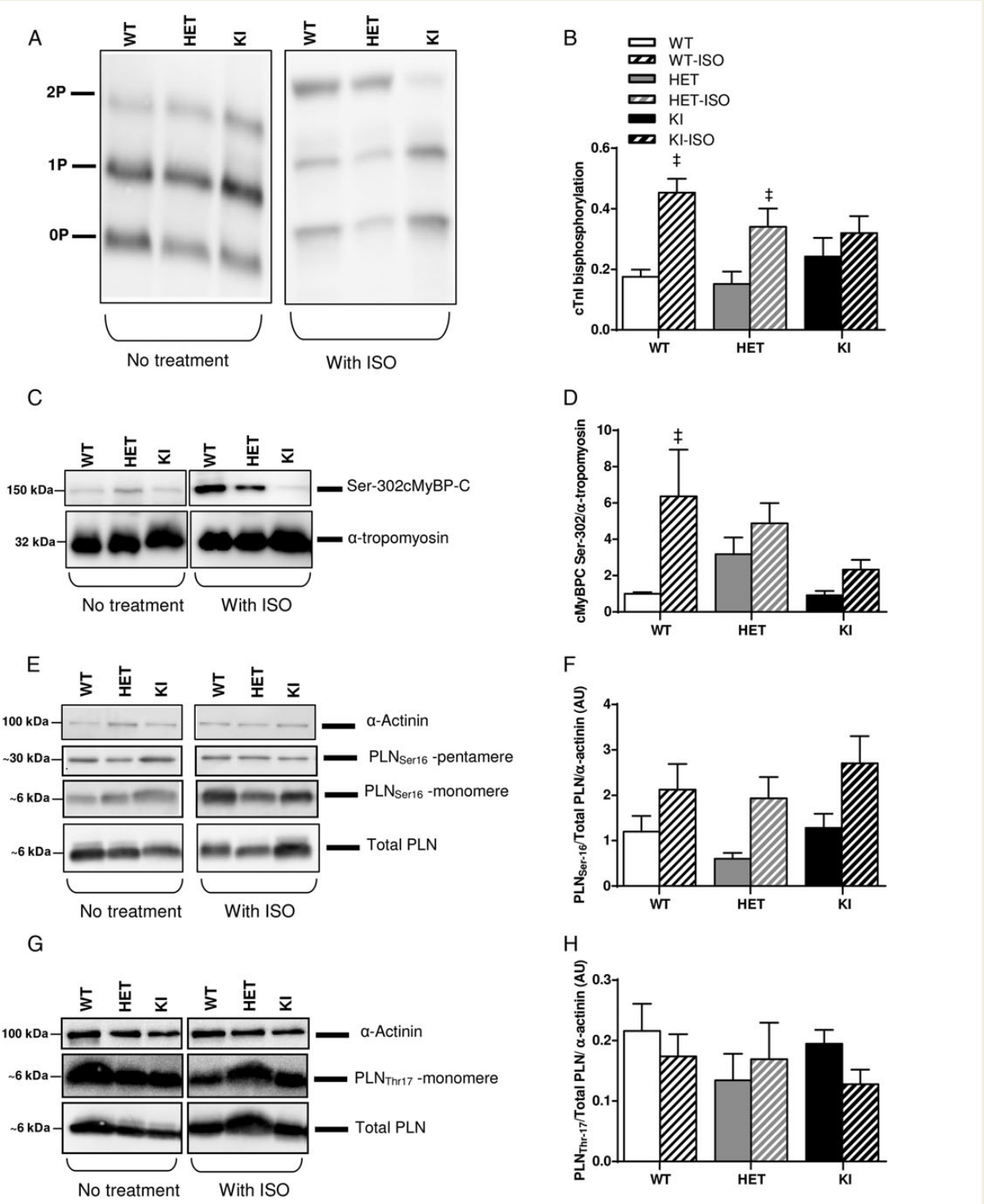

Figure 6 Cardiomyocyte phospholamban (PLN), but not cTnI and cMyBP-C phosphorylation, increased with ISO treatment. (*A*) The distribution of phosphorylated forms of cTnI is illustrated using phos-tag acrylamide gel. (*B*) The relative fraction of bisphosphorylated form (2P) of cTnI was significantly increased in WT [number of mice (*N*) = 10] and HET KI (*N* = 9) upon ISO perfusion, although remained unchanged in homozygous KI (*N* = 9) mice. (*C*) Western blot analysis of cMyBP-C, normalized for the loading control α-tropomyosin, was performed after ISO treatment. The values from WT cells, without ISO treatment, were set as 1. (*D*) A significant increase in serine (Ser)-302 phosphorylation of cMyBP-C was particularly found in WT (*N* = 3; HET: *N* = 3; KI: *N* = 4) cardiomyocytes upon ISO treatment, compared with untreated cardiomyocytes, which was set as 1. (*E*) The phosphorylated isoforms of PLN Ser-16 in untreated cells and after ISO are separately normalized for total PLN and the loading control α-actinin and finally summed up as one PLN phosphorylation value per mouse. (*F*) In contrast, PLN Ser-16 phosphorylation in KI (*N* = 9) was similar to the WT (*N* = 12) and HET (*N* = 8) values after ISO ($P_{treatment} < 0.05$ in two-way ANOVA). No changes in threonine (Thr)-17 phosphorylation has been found in KI (*N* = 7) and HET (*N* = 7) mice before and after ISO, compared with the corresponding WT (*N* = 11). $^{‡}P < 0.05$ vs. corresponding to untreated mice in two-way ANOVA.

PKA-mediated decrease in myofilament Ca^{2+} sensitivity was maximal at ~55% bisphosphorylated cTnI. Similar findings were observed in PKA-treated cardiomyocytes obtained from HCM patients who underwent myectomy surgery as well as studies in transgenic HCM mouse models.[9,12] PKA pre-treatment also normalized the high F_{pas} in KI to the WT values, which might indicate a lower PKA-mediated phosphorylation of titin in KI mice. It is known that PKA (as well as protein kinase G) phosphorylation of titin reduces the resting tension, whereas protein kinase C titin phosphorylation predominantly increases passive tension.[27] A drawback of the current technique is that we could not distinguish between different phosphorylation sites, and we therefore cannot exclude that compensatory changes (e.g. more PKC and less PKA phosphorylation of titin) might contribute to changes in passive stiffness in our mouse model (*Figure 2C*). A possible explanation for the reduced myofilament phosphorylation and consequently higher myofilament Ca^{2+} sensitivity and F_{pas} may reside in impaired β-AR signalling cascade. We have previously reported the increased myofilament Ca^{2+} sensitivity in patients with HCM, in which the majority developed less force compared with donors.[9,32,33] In this study, we showed a higher passive tension and high basal activation at low calcium levels in KI cardiomyocytes, which might affect myocardial relaxation and reduce the Frank–Starling reserve. The low resting SL in intact KI cardiomyocytes before and after ISO treatment is indicative for high basal activation. A possible contributor to high resting tension is residual cross-bridge attachment. In a cMyBP-C knock-out mouse model, the cross-bridge inhibitor 2,3-butanedione monoxime was shown to increase diastolic SL, indicating that some residual cross-bridge attachment occurs in permeabilized cardiomyocytes at low Ca^{2+}.[34] We have also recently shown that the cross-bridge component might be a more important component to resting or passive tension than previously thought.[35] Noteworthy, the myofilament contraction does not seem to be affected by low basal SL in KI mice as it there was no correlation between resting SL and sarcomere shortening, demonstrated in the Supplementary material online, *Figure S7*.

In addition to KI mice, it should also be mentioned that despite reduced expression of cMyBP-C in KI mice, maximal ktr was similar in permeabilized cardiomyocytes from KI and WT mice. Reduced cMyBP-C expression will release the brake on myosin heads and increase the rate of force development. However, small disease-related changes in MHC isoform may also alter the rate of force development.[36,37] MHC isoform analysis (Supplementary material online, *Figure S6A* and *B*) revealed a significant increase in β-MHC (i.e. a slow isoform of MHC) in KI mice, indicating that an effect of reduced cMyBP-C expression on speed of force re-development may be counterbalanced by the expression of slow β-MHC isoform in KI mice.

Normalization of myofilament Ca^{2+} sensitivity and F_{pas} after PKA incubation in KI mice indicates a relatively limited direct contribution of cMyBP-C in the regulation of myofilament Ca^{2+} sensitivity and passive tension. There is still much debate on the role that cMyBP-C plays in modulating Ca^{2+} sensitivity. This is illustrated by the diverse effects seen in the different cMyBP-C protein null mouse models: Harris *et al.*[38] showed that Ca^{2+} sensitivity decreased in cMyBP-C KO, Fraysse *et al.*[22] showed in a different model without functional cMyBP-C that Ca^{2+} sensitivity increased, and Barefield *et al.*[39] showed no change in Ca^{2+} sensitivity. In a number of studies from our group, we have shown that in cardiac tissue from HCM patients, low levels of cMyBP-C do not directly mediate myofilament calcium sensitivity,[9,10,32,33] but changes in Ca^{2+} sensitivity occur due to secondary remodelling. The most important determinant in the regulation of myofilament Ca^{2+} sensitivity of force development is phosphorylation of myofilament targets, particularly cTnI.[29] This is supported by our data which show that restoring the low cTnI phosphorylation level can normalize myofilament Ca^{2+} sensitivity and that this overrules any role that cMyBP-C might play in modulating Ca^{2+} sensitivity.

Noteworthy, our previous study in patients with an *MYBPC3* missense mutation revealed a pattern of protein phosphorylation similar to the truncated *MYBPC3* mutation group,[9] indicating that the β-AR pathway might be affected to a similar degree, regardless of the type of mutation. Recent findings also seem to indicate that the distinction between missense and truncation mutations is not as black and white as previously thought. Even in patients with missense mutations, a reduced level of cMyBP-C was found, which might be caused by decreased stability of the mutant protein.[40,41] Besides carrying different types of mutations, it is important to note that the protein expression level may contribute to the disturbed β-AR pathway. Previously, we provided evidence that mutant protein may impair sarcomere function at ~38% expression,[9] which emphasizes the importance of studying the WT and mutant protein level at which myofilament protein phosphorylation and performance are impaired.

4.2 Reduced FSL relation in HET and KI cardiomyocytes

In KI mice, the slope of diastolic FSL relation of intact isolated cardiomyocytes seems to be unaltered (*Figure 4D*), whereas a shorter SL (*Figure 5A*) and a higher passive tension in these permeabilized cells were measured (*Figure 2A*), compared with WT. The difference in passive tension between KI and WT mice became apparent at SL ≥ 2.0 μm in permeabilized cardiomyocytes. In loaded intact cells, we were able to determine the FSL relation at the SL range ~1.7–1.9 μm. Therefore, we might have seen a higher diastolic FSL in intact KI cardiomyocytes if we would have stretched cells beyond SL 2.0 μm. Another factor that might influence our measurements was the inability to normalize absolute force development for cross-sectional area in an intact cell. To circumvent this problem, we used the ratio of systolic over diastolic slope of FSL relation.

We calculate the slope of diastolic and systolic FSL relations obtained by varying the pre-load (i.e. stretching the single intact cell). It has been previously reported that the FSL relation in mammals is near linear at SL 1.85–2.05 μm.[21,42] Our loaded intact cardiomyocytes revealed a significantly lower systolic/diastolic ratio of FSL relation in both HET and KI than in WT mice within the range of studied SL values, suggesting less tension production per unit increase in SL (*Figure 4F*). This finding in loaded intact cells is in contrast to our permeabilized cardiomyocyte data, in which an increase in SL (from 1.8 to 2.2 μm) elevated the maximal generated tension similarly in all groups (*Figure 2C* and *E* and *Table 1*). The difference between LDA response in intact and permeabilized cardiomyocytes could be explained by the presence of intracellular Ca^{2+}-handling machinery, whereas in permeabilized cardiomyocytes, all organelles are removed and the [Ca^{2+}] is manually regulated. We observed in membrane-permeabilized cardiomyocytes a higher F_{pas} in KI-isolated cells. However, the diastolic FSL relation in intact cardiomyocytes remained unchanged between the groups. Several factors such as temperature, pH, and experiment medium may explain differences between membrane-permeabilized and intact cardiomyocytes. Noteworthy, the SL range in intact cardiomyocytes was lower (~1.7–1.9 μm) compared with that in permeabilized cardiomyocytes (1.8–2.2 μm), which also might underlie the discrepancy between

intact and permeabilized cells. It is important to mention that in permeabilized cardiomyocytes of KI mice, we observed that myofilaments were sensitized to Ca^{2+} ions (i.e. myofilament effect), whereas in intact cardiomyocytes, we did not find changes in Ca^{2+} handling (i.e. sarcoplasmic reticulum effect) compared with WT. This suggests that the Ca^{2+}-handling function in KI is preserved, whereas there is an increased myofilament Ca^{2+} sensitivity. Taking together, our data indicate a mildly blunted increase in myofilament Ca^{2+} sensitivity upon stretch in membrane-permeabilized cardiomyocytes from KI mice, whereas intact cardiomyocytes showed an impaired length-dependent cardiomyocyte activation in HET and KI mice.

4.3 Blunted cardiomyocyte response to ISO with preserved Ca^{2+} handling

β-AR receptor stimulation activates adenylyl cyclase, which catalyses the synthesis of cyclic adenosine monophosphate (cAMP) from ATP. cAMP binds to regulatory subunits of the PKA holoenzyme complex, leading to conformational changes and release of the PKAcat subunit of PKA. Our results indicate blunted myofilament β-AR response to ISO in KI. However, the increase in Ca^{2+} transients after ISO was unchanged between the groups. This suggests preferential β-AR signalling to the SR over the myofilament in KI. It is important to note that the baseline phosphorylation state was similar between KI and WT mice (*Figure 6*), indicating that the baseline inotropic state is probably comparable between the groups, and leading subsequently in KI mice with ISO treatment to an attenuated β-AR response.

A reduced response upon β-AR stimulation was also reported in hearts from cMyBP-C knock-out mice.[43] Another study in the Mybpc3 transgenic mouse model, using PKA-dependent back phosphorylation assay, revealed a reduced cTnI as well as PLN phosphorylation.[44] In this study, we found a preserved Ca^{2+} handling, despite an attenuated cTnI and Ser-302 cMyBP-C phosphorylation after ISO treatment in KI mice. In our experiments, we did not see reduced PKAcat expression (Supplementary material online, *Figure S1B*), but observed selective targeting of PKA to the SR. Interestingly, our findings in KI mice regarding the attenuated myofilament response upon ISO did not appear to result in alterations in Ca^{2+} transients of the cell. This might appear in contrast to a recent study which indicated that the inability to phosphorylate cTnI and lower myofilament Ca^{2+} buffering following ISO treatment results in a decreased Ca^{2+}-transient amplitude.[45] The latter study was performed in mice carrying TnI, which could not be phosphorylated by PKA. The lack of an effect on calcium transients in our KI model may be explained by the degree of cTnI phosphorylation, which may still be sufficiently high.

The differential response upon β-AR stimulation in this study between the myofilament and Ca^{2+}-handling systems was confirmed by protein phosphorylation data (preserved PLN phosphorylation increase and attenuated cTnI phosphorylation increase).

4.4 Low myofilament phosphorylation upon ISO

Selective phosphorylation of PKA targets was also confirmed by our protein analyses. In LV frozen tissue, a significantly lower cTnI, but a preserved PLN phosphorylation was seen in KI mice when compared with WT (Supplementary material online, *Figure S3A* and *B*). This suggests that phosphorylation of PLN is preferential over cTnI *in vivo*. Upon ISO treatment, cTnI bisphosphorylation and cMyBP-C Ser-302 failed to increase in KI cardiomyocytes, whereas PLN phosphorylation increased to an equal extent in all groups (*Figure 6A–F*).

It should also be noted that cTnI phosphorylation in KI was significantly lower in LV frozen tissue compared with WT, which was not seen in the isolated cells at baseline. This experimental discrepancy is caused by loss of protein phosphorylation, particularly in WT cardiomyocytes, during the isolation procedure. This artefact is an important factor to keep in mind when performing isolated cardiomyocyte experiments. The LV frozen data in our opinion closely reflect the situation in the *in vivo* heart. The experiments performed in the intact isolated cells exposed to ISO were used to assess the ability of β-AR stimulation to signal downstream to cTnI and PLN.

The selective signalling to one compartment (SR) over another (myofilaments) could be explained by changes in PKA localization. This localization of PKA is achieved by docking of PKA near substrates, which is mediated by AKAPs.[17,46] Binding of the PKA complex to these AKAPs occurs through the regulatory subunits. Two major forms of PKA complexes have been described. These two types differ in their structure in the regulatory subunit of the PKA complex, termed as PKA-RI (PKA regulatory subunit I) and PKA-RII,[46] both of which bind to the same PKAcat subunit. A higher PKA-RI, but unchanged PKAcat subunit expression, has been reported in failing human myocardial tissue,[47] indicating that during HF PKA subunits may not be expressed in matched quantities. Similarly, in the present study, a higher PKA-RII and an unchanged PKAcat expression were detected in KI mice (Supplementary material online, *Figure S1*).

Another important phenomenon is high oxidative stress in patients with HCM,[48] which may result in oxidation of many proteins, among which the regulatory subunit of PKA. A study by Brennan *et al.*[49] showed that oxidation of the two regulatory RI units in response to H_2O_2 may cause a subcellular translocation and activation of the kinase, resulting in the phosphorylation of target proteins. The translocation, as the authors indicated, is partially mediated by the oxidized form of the kinase having an enhanced affinity for alpha-MHC, which serves as an AKAP and localizes PKA to the myofilament substrates. Taken together, selective phosphorylation of PLN over myofilament proteins and preserved Ca^{2+} homeostasis in KI mice after ISO treatment may possibly be caused by a maintained PKA localization towards the SR, resulting in a preserved PLN, but lower myofilament protein phosphorylation (Supplementary material online, *Figure S4*).

4.5 Conclusion and clinical implications

The HCM-associated mouse model carrying a G > A transition on the last nucleotide of exon 6 showed similar cellular changes as observed in previous studies in cardiac samples from HCM patients with a known mutation in the gene encoding cMyBP-C such as reduced expression of mutant protein, low PKA-mediated myofilament protein phosphorylation, increased Ca^{2+} sensitivity, and perturbed LDA.[9,33] Our study confirmed an increased Ca^{2+} sensitivity and a reduced cardiomyocyte contractile performance in KI mice. It seems that a post-translational modification (such as reduced myofilament protein phosphorylation) in KI mice and HCM patients with MYBPC3 mutations is one of the major mechanisms of altered myocardial function. The data presented in this study show that PKA hypophosphorylation can explain the observed contractile dysfunction. However, simply increasing PKA phosphorylation by reduced desensitization or other strategies is likely not sufficient as the localization of PKA signalling needs to be addressed. AKAPs are important modulators in spatial and temporal control of cellular signalling. Alterations in AKAP interaction and/or expression

are associated with cardiac pathologies.[17] This suggests that complete understanding of AKAP–PKA complexes and their function in heart disease might be interesting targets for the treatment of cardiomyopathy.[50]

Supplementary material

Supplementary material is available at *Cardiovascular Research* online.

Acknowledgements

We are grateful to Saskia Schlossarek for organizing and supplying us with *Mybpc3*-targeted KI mice and for valuable support. We thank Sakthivel Sadayappan from Department of Cell and Molecular Physiology, Health Sciences Division, Loyola University Chicago for supplying us with cMyBP-C Ser-302 antibody.

Conflict of interest: none declared.

Funding

We acknowledge support from the Netherlands Organization for Scientific Research (NWO; VIDI grant 91711344), the 7th Framework Program of the European Union ('BIG-HEART', grant agreement no. 241577), and the ICIN—Netherlands Heart Institute.

References

1. Semsarian C, Ingles J, Maron MS, Maron BJ. New perspectives on the prevalence of hypertrophic cardiomyopathy. *J Am Coll Cardiol* 2015;**65**:1249–1254.
2. Tardiff JC, Carrier L, Bers DM, Poggesi C, Ferrantini C, Coppini R, Maier LS, Ashrafian H, Huke S, van der Velden J. Targets for therapy in sarcomeric cardiomyopathies. *Cardiovasc Res* 2015;**105**:457–470.
3. Alcalai R, Seidman JG, Seidman CE. Genetic basis of hypertrophic cardiomyopathy: from bench to the clinics. *J Cardiovasc Electrophysiol* 2008;**19**:104–110.
4. Hershberger RE, Cowan J, Morales A, Siegfried JD. Progress with genetic cardiomyopathies: screening, counseling, and testing in dilated, hypertrophic, and arrhythmogenic right ventricular dysplasia/cardiomyopathy. *Circ Heart Fail* 2009;**2**:253–261.
5. Richard P, Charron P, Carrier L, Ledeuil C, Cheav T, Pichereau C, Benaiche A, Isnard R, Dubourg O, Burban M, Gueffet JP, Millaire A, Desnos M, Schwartz K, Hainque B, Komajda M. Hypertrophic cardiomyopathy: distribution of disease genes, spectrum of mutations, and implications for a molecular diagnosis strategy. *Circulation* 2003;**107**:2227–2232.
6. Eschenhagen T. Beta-adrenergic signaling in heart failure—adapt or die. *Nat Med* 2008;**14**:485–487.
7. Schumacher C, Becker H, Conrads R, Schotten U, Pott S, Kellinghaus M, Sigmund M, Schondube F, Preusse C, Schulte HD, Hanrath P. Hypertrophic cardiomyopathy: a desensitized cardiac beta-adrenergic system in the presence of normal plasma catecholamine concentrations. *Naunyn Schmiedebergs Arch Pharmacol* 1995;**351**:398–407.
8. Choudhury L, Guzzetti S, Lefroy DC, Nihoyannopoulos P, McKenna WJ, Oakley CM, Camici PG. Myocardial beta adrenoceptors and left ventricular function in hypertrophic cardiomyopathy. *Heart* 1996;**75**:50–54.
9. Sequeira V, Wijnker PJ, Nijenkamp LL, Kuster DW, Najafi A, Witjas-Paalberends ER, Regan JA, Boontje N, Ten Cate FJ, Germans T, Carrier L, Sadayappan S, van Slegtenhorst MA, Zaremba R, Foster DB, Murphy AM, Poggesi C, Dos Remedios C, Stienen GJ, Ho CY, Michels M, van der Velden J. Perturbed length-dependent activation in human hypertrophic cardiomyopathy with missense sarcomeric gene mutations. *Circ Res* 2013;**112**:1491–1505.
10. van Dijk SJ, Dooijes D, dos Remedios C, Michels M, Lamers JM, Winegrad S, Schlossarek S, Carrier L, ten Cate FJ, Stienen GJ, van der Velden J. Cardiac myosin-binding protein C mutations and hypertrophic cardiomyopathy: haploinsufficiency, deranged phosphorylation, and cardiomyocyte dysfunction. *Circulation* 2009;**119**:1473–1483.
11. Koss KL, Kranias EG. Phospholamban: a prominent regulator of myocardial contractility. *Circ Res* 1996;**79**:1059–1063.
12. Stelzer JE, Patel JR, Walker JW, Moss RL. Differential roles of cardiac myosin-binding protein C and cardiac troponin I in the myofibrillar force responses to protein kinase a phosphorylation. *Circ Res* 2007;**101**:503–511.
13. Kuster DW, Bawazeer AC, Zaremba R, Goebel M, Boontje NM, van der Velden J. Cardiac myosin binding protein C phosphorylation in cardiac disease. *J Muscle Res Cell Motil* 2012;**33**:43–52.
14. Schmidt U, Hajjar RJ, Kim CS, Lebeche D, Doye AA, Gwathmey JK. Human heart failure: cAMP stimulation of SR Ca(2+)-ATPase activity and phosphorylation level of phospholamban. *Am J Physiol* 1999;**277**:H474–H480.
15. Schulz EM, Wilder T, Chowdhury SA, Sheikh HN, Wolska BM, Solaro RJ, Wieczorek DF. Decreasing tropomyosin phosphorylation rescues tropomyosin-induced familial hypertrophic cardiomyopathy. *J Biol Chem* 2013;**288**:28925–28935.
16. Freeman K, Colon-Rivera C, Olsson MC, Moore RL, Weinberger HD, Grupp IL, Vikstrom KL, Iaccarino G, Koch WJ, Leinwand LA. Progression from hypertrophic to dilated cardiomyopathy in mice that express a mutant myosin transgene. *Am J Physiol Heart Circ Physiol* 2001;**280**:H151–H159.
17. Ruehr ML, Russell MA, Bond M. A-kinase anchoring protein targeting of protein kinase A in the heart. *J Mol Cell Cardiol* 2004;**37**:653–665.
18. Vignier N, Schlossarek S, Fraysse B, Mearini G, Kramer E, Pointu H, Mougenot N, Guiard J, Reimer R, Hohenberg H, Schwartz K, Vernet M, Eschenhagen T, Carrier L. Nonsense-mediated mRNA decay and ubiquitin–proteasome system regulate cardiac myosin-binding protein C mutant levels in cardiomyopathic mice. *Circ Res* 2009;**105**:239–248.
19. Warren CM, Jordan MC, Roos KP, Krzesinski PR, Greaser ML. Titin isoform expression in normal and hypertensive myocardium. *Cardiovasc Res* 2003;**59**:86–94.
20. McKee LA, Chen H, Regan JA, Behunin SM, Walker JW, Walker JS, Konhilas JP. Sexually dimorphic myofilament function and cardiac troponin I phosphospecies distribution in hypertrophic cardiomyopathy mice. *Arch Biochem Biophys* 2012;**535**:39–48.
21. King NM, Methawasin M, Nedrud J, Harrell N, Chung CS, Helmes M, Granzier H. Mouse intact cardiac myocyte mechanics: cross-bridge and titin-based stress in unactivated cells. *J Gen Physiol* 2011;**137**:81–91.
22. Fraysse B, Weinberger F, Bardswell SC, Cuello F, Vignier N, Geertz B, Starbatty J, Kramer E, Coirault C, Eschenhagen T, Kentish JC, Avkiran M, Carrier L. Increased myofilament Ca2+ sensitivity and diastolic dysfunction as early consequences of Mybpc3 mutation in heterozygous knock-in mice. *J Mol Cell Cardiol* 2012;**52**:1299–1307.
23. Najafi A, Schlossarek S, van Deel ED, van den Heuvel N, Guclu A, Goebel M, Kuster DW, Carrier L, van der Velden J. Sexual dimorphic response to exercise in hypertrophic cardiomyopathy-associated Mybpc3-targeted knock-in mice. *Pflugers Arch* 2015;**467**:1303–1317.
24. Cazorla O, Szilagyi S, Vignier N, Salazar G, Kramer E, Vassort G, Carrier L, Lacampagne A. Length and protein kinase A modulations of myocytes in cardiac myosin binding protein C-deficient mice. *Cardiovasc Res* 2006;**69**:370–380.
25. Ho CY, Sweitzer NK, McDonough B, Maron BJ, Casey SA, Seidman JG, Seidman CE, Solomon SD. Assessment of diastolic function with Doppler tissue imaging to predict genotype in preclinical hypertrophic cardiomyopathy. *Circulation* 2002;**105**:2992–2997.
26. Braunwald E, Lambrew CT, Rockoff SD, Ross J Jr, Morrow AG. Idiopathic hypertrophic subaortic stenosis. I. A description of the disease based upon an analysis of 64 patients. *Circulation* 1964;**30**:3–119.
27. Yamasaki R, Wu Y, McNabb M, Greaser M, Labeit S, Granzier H. Protein kinase A phosphorylates titin's cardiac-specific N2B domain and reduces passive tension in rat cardiac myocytes. *Circ Res* 2002;**90**:1181–1188.
28. McKee LA, Chen H, Regan JA, Behunin SM, Walker JW, Walker JS, Konhilas JP. Sexually dimorphic myofilament function and cardiac troponin I phosphospecies distribution in hypertrophic cardiomyopathy mice. *Arch Biochem Biophys* 2013;**535**:39–48.
29. de Tombe PP, Stienen GJ. Protein kinase A does not alter economy of force maintenance in skinned rat cardiac trabeculae. *Circ Res* 1995;**76**:734–741.
30. Wijnker PJ, Foster DB, Tsao AL, Frazier AH, dos Remedios CG, Murphy AM, Stienen GJ, van der Velden J. Impact of site-specific phosphorylation of protein kinase A sites Ser23 and Ser24 of cardiac troponin I in human cardiomyocytes. *Am J Physiol Heart Circ Physiol* 2013;**304**:H260–H268.
31. Wijnker PJ, Murphy AM, Stienen GJ, van der Velden J. Troponin I phosphorylation in human myocardium in health and disease. *Neth Heart J* 2014;**22**:463–469.
32. Witjas-Paalberends ER, Piroddi N, Stam K, van Dijk SJ, Oliviera VS, Ferrara C, Scellini B, Hazebroek M, ten Cate FJ, van Slegtenhorst M, dos Remedios C, Niessen HW, Tesi C, Stienen GJ, Heymans S, Michels M, Poggesi C, van der Velden J. Mutations in MYH7 reduce the force generating capacity of sarcomeres in human familial hypertrophic cardiomyopathy. *Cardiovasc Res* 2013;**99**:432–441.
33. van Dijk SJ, Paalberends ER, Najafi A, Michels M, Sadayappan S, Carrier L, Boontje NM, Kuster DW, van Slegtenhorst M, Dooijes D, dos Remedios C, ten Cate FJ, Stienen GJ, van der Velden J. Contractile dysfunction irrespective of the mutant protein in human hypertrophic cardiomyopathy with normal systolic function. *Circ Heart Fail* 2012;**5**:36–46.
34. Pohlmann L, Kroger I, Vignier N, Schlossarek S, Kramer E, Coirault C, Sultan KR, El-Armouche A, Winegrad S, Eschenhagen T, Carrier L. Cardiac myosin-binding protein C is required for complete relaxation in intact myocytes. *Circ Res* 2007;**101**:928–938.
35. Sequeira V, Najafi A, McConnell M, Fowler ED, Bollen IA, Wust RC, dos Remedios C, Helmes M, White E, Stienen GJ, Tardiff J, Kuster DW, van der Velden J. Synergistic role of ADP and Ca(2+) in diastolic myocardial stiffness. *J Physiol* 2015;**593**:3899–3916.
36. Eiras S, Narolska NA, van Loon RB, Boontje NM, Zaremba R, Jimenez CR, Visser FC, Stooker W, van der Velden J, Stienen GJ. Alterations in contractile protein composition and function in human atrial dilatation and atrial fibrillation. *J Mol Cell Cardiol* 2006;**41**:467–477.
37. Narolska NA, Eiras S, van Loon RB, Boontje NM, Zaremba R, Spiegelen Berg SR, Stooker W, Huybregts MA, Visser FC, van der Velden J, Stienen GJ. Myosin heavy chain composition and the economy of contraction in healthy and diseased human myocardium. *J Muscle Res Cell Motil* 2005;**26**:39–48.

38. Harris SP, Bartley CR, Hacker TA, McDonald KS, Douglas PS, Greaser ML, Powers PA, Moss RL. Hypertrophic cardiomyopathy in cardiac myosin binding protein-C knockout mice. *Circ Res* 2002;**90**:594–601.
39. Barefield D, Kumar M, de Tombe PP, Sadayappan S. Contractile dysfunction in a mouse model expressing a heterozygous MYBPC3 mutation associated with hypertrophic cardiomyopathy. *Am J Physiol Heart Circ Physiol* 2014;**306**:H807–H815.
40. Marston S, Copeland O, Jacques A, Livesey K, Tsang V, McKenna WJ, Jalilzadeh S, Carballo S, Redwood C, Watkins H. Evidence from human myectomy samples that MYBPC3 mutations cause hypertrophic cardiomyopathy through haploinsufficiency. *Circ Res* 2009;**105**:219–222.
41. Sequeira V, Najafi A, Wijnker PJ, Dos Remedios CG, Michels M, Kuster DW, van der Velden J. Adp-stimulated contraction: a predictor of thin-filament activation in cardiac disease. *Proc Natl Acad Sci USA* 2015;**112**:E7003–E7012.
42. Iribe G, Helmes M, Kohl P. Force–length relations in isolated intact cardiomyocytes subjected to dynamic changes in mechanical load. *Am J Physiol Heart Circ Physiol* 2007; **292**:H1487–H1497.
43. Carrier L, Knoll R, Vignier N, Keller DI, Bausero P, Prudhon B, Isnard R, Ambroisine ML, Fiszman M, Ross J Jr., Schwartz K, Chien KR. Asymmetric septal hypertrophy in heterozygous cMyBP-C null mice. *Cardiovasc Res* 2004;**63**:293–304.
44. Yang Q, Hewett TE, Klevitsky R, Sanbe A, Wang X, Robbins J. PKA-dependent phosphorylation of cardiac myosin binding protein C in transgenic mice. *Cardiovasc Res* 2001; **51**:80–88.
45. Briston SJ, Dibb KM, Solaro RJ, Eisner DA, Trafford AW. Balanced changes in Ca buffering by SERCA and troponin contribute to Ca handling during beta-adrenergic stimulation in cardiac myocytes. *Cardiovasc Res* 2014;**104**:347–354.
46. Dwivedi Y, Pandey GN. Adenylyl cyclase-cyclicAMP signaling in mood disorders: role of the crucial phosphorylating enzyme protein kinase A. *Neuropsychiatr Dis Treat* 2008;**4**: 161–176.
47. Han YS, Arroyo J, Ogut O. Human heart failure is accompanied by altered protein kinase A subunit expression and post-translational state. *Arch Biochem Biophys* 2013;**538**: 25–33.
48. Dimitrow PP, Undas A, Wolkow P, Tracz W, Dubiel JS. Enhanced oxidative stress in hypertrophic cardiomyopathy. *Pharmacol Rep* 2009;**61**:491–495.
49. Brennan JP, Bardswell SC, Burgoyne JR, Fuller W, Schroder E, Wait R, Begum S, Kentish JC, Eaton P. Oxidant-induced activation of type I protein kinase A is mediated by RI subunit interprotein disulfide bond formation. *J Biol Chem* 2006;**281**:21827–21836.
50. Troger J, Moutty MC, Skroblin P, Klussmann E. A-kinase anchoring proteins as potential drug targets. *Br J Pharmacol* 2012;**166**:420–433.